Ma et al. BMC Genomics (2019) 20:655
https://doi.org/10.1186/s12864-019-6030-5

BMC Genomics

RESEARCH ARTICLE Open Access

ITRAQ-based proteomic analysis reveals possible target-related proteins in human adrenocortical adenomas

He Ma[1,5†], Ranwei Li[2†], Xin Di[1], Xin Jin[3], Yan Wang[1], Bingjie Lai[4], Cailian Shi[5], Mingxin Ji[5], Xinran Zhu[5] and Ke Wang[1*]

Abstract

Background: Adrenocortical adenomas (ACAs) can lead to the autonomous secretion of aldosterone responsible for primary aldosteronism (PA), which is the most common form of secondary arterial hypertension. However, the authentic fundamental mechanisms underlying ACAs remain unclear.

Objective: Isobaric tags for relative and absolute quantitation (iTRAQ)-based proteomics and bioinformatics analyses from etiological studies of ACAs were performed to screen the differentially expressed proteins (DEPs) and investigate the relevant mechanisms of their occurrence and development. Results could help determine therapeutic targets of clinical significance.

Methods: In the present study, iTRAQ-based proteomics was applied to analyze ACA tissue samples from normal adrenal cortex tissues adjacent to the tumor. Using proteins extracted from a panel of four pairs of ACA samples, we identified some upregulated proteins and other downregulated proteins in all four pairs of ACA samples compared with adjacent normal tissue. Subsequently, we predicted protein–protein interaction networks of three DEPs to determine the authentic functional factors in ACA.

Results: A total of 753 DEPs were identified, including 347 upregulated and 406 downregulated proteins. The expression of three upregulated proteins (E2F3, KRT6A, and ALDH1A2) was validated by Western blot in 24 ACA samples. Our data suggested that some DEPs might be important hallmarks during the development of ACA.

Conclusions: This study is the first proteomic research to investigate alterations in protein levels and affected pathways in ACA using the iTRAQ technique. Thus, this study not only provides a comprehensive dataset on overall protein changes but also sheds light on its potential molecular mechanism in human ACAs.

Keywords: iTRAQ, Adrenocortical adenoma, Proteomics, Differentially expressed protein

Background

Primary aldosteronism (PA) is considered the most common cause of endocrine hypertension [1, 2]; it occurs in approximately 10–20% of hypertensive patients. Adrenocortical adenomas (ACAs) can lead to the autonomous secretion of aldosterone responsible for PA [3], which is the most frequent form of secondary arterial hypertension [4, 5]. Even though previous proteomic studies have already focused on differentially expressed proteins (DEPs) and made adequate progress in the understanding of the genetic bases of aldosterone- and cortisol-producing ACAs in the past few years [6–8], the authentic molecular mechanism and fundamental biological activities of DEPs underlying ACA remain ambiguous.

Additionally, quantitative proteomics, as an important methodology based on mass spectrometry, is widely used in the biological and clinical research of various diseases, such as the monitoring of specific disease biomarkers or the identification of functional modules and pathways [9–12]. Bioinformatic analysis of the dynamic transcriptome and expression regulation may guide future

* Correspondence: kewangm1@hotmail.com
†He Ma and Ranwei Li contributed equally to this work.
[1]Department of Respiratory Medicine, the Second Hospital of Jilin University, Changchun, China
Full list of author information is available at the end of the article

research on the mechanisms of ACA. Both isobaric tags for relative and absolute quantitation (iTRAQ) and label-free methods have been broadly applied for quantitative proteomics [13–16]. These techniques are compatible with high-throughput and high speed and can improve the reproducibility of prefractionation of complex peptide mixtures [17–19]. Nevertheless, proteomic studies about ACA are limited. Establishing differentially expressed protein–protein interaction (PPI) networks using bioinformatic data will lead to an improved understanding of the pathogenesis of ACA.

In this work, iTRAQ-based proteomic analysis was conducted based on the etiological study of adrenal adenoma to screen DEPs and explore the relevant mechanisms of its occurrence and development. Results of this study may be used to determine therapeutic targets of clinical significance, which might lay a theoretical foundation for the early diagnosis and effective treatment of adrenal adenoma.

Results

In this study, iTRAQ was used to assess proteome changes between adrenocortical adenoma tissue and adjacent normal adrenal cortex tissue. On the basis of data acquisition, 753 DEPs were identified: 347 upregulated and 9406 downregulated proteins.

Gene ontology (GO) analysis results

GO is a standardized functional classification system that provides a dynamically updated standardized vocabulary to describe the properties of genes and gene products in an organism from three perspectives: biological process, molecular function, and cell component [20] (Fig. 1).

The GO annotation of target proteins can classify these involved proteins in terms of biological process, molecular function, and cellular component (Fig. 2). Although the proportion of each classification can reflect the impact of biological factors on each classification in the experimental design to a certain extent, evaluations on the significance of each classification depending on the ratio alone are inaccurate. Notably, the distributions of each classification should be considered in overall protein collection, such as all qualitative proteins in an experiment or all known proteins of the species.

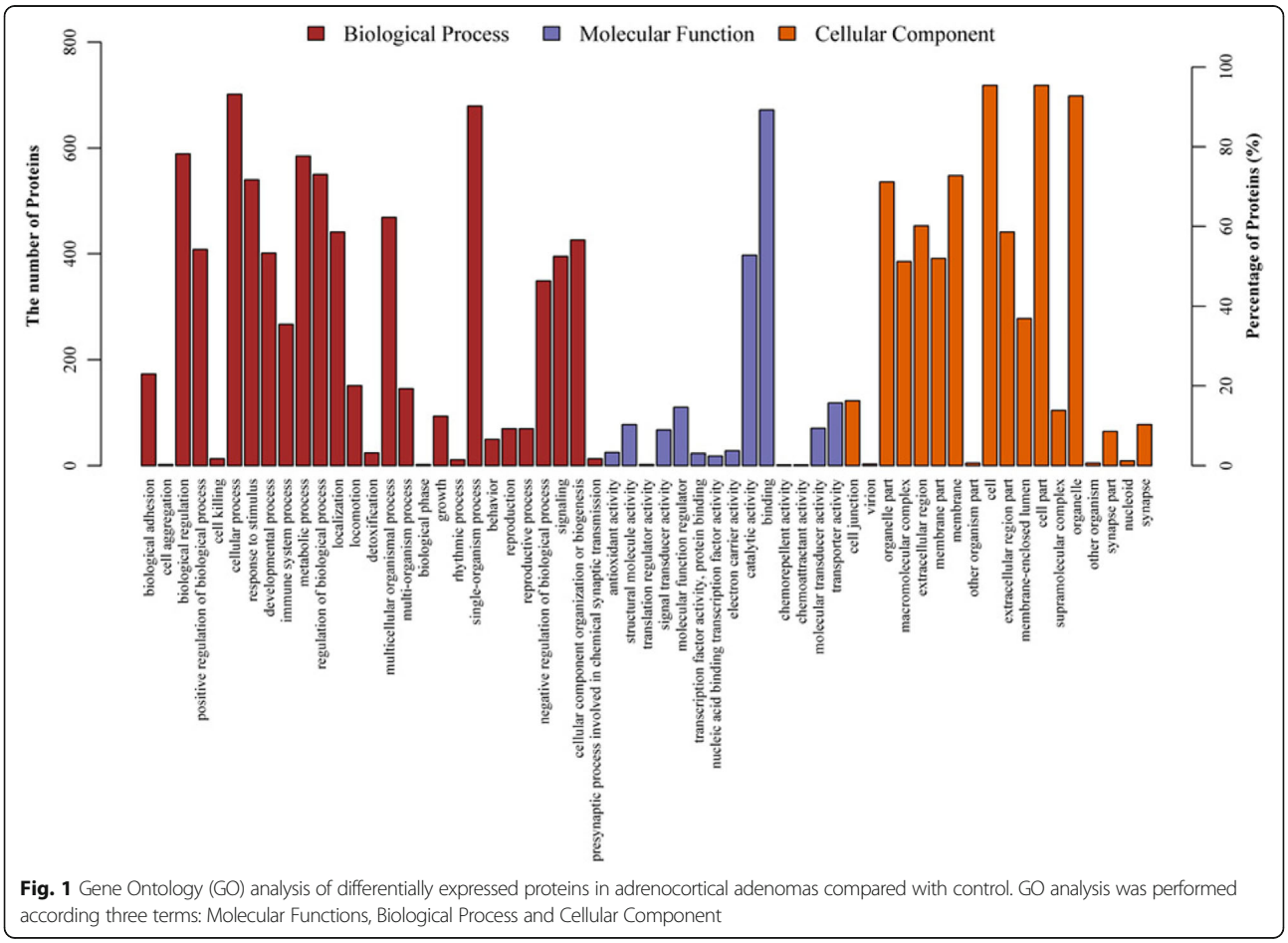

Fig. 1 Gene Ontology (GO) analysis of differentially expressed proteins in adrenocortical adenomas compared with control. GO analysis was performed according three terms: Molecular Functions, Biological Process and Cellular Component

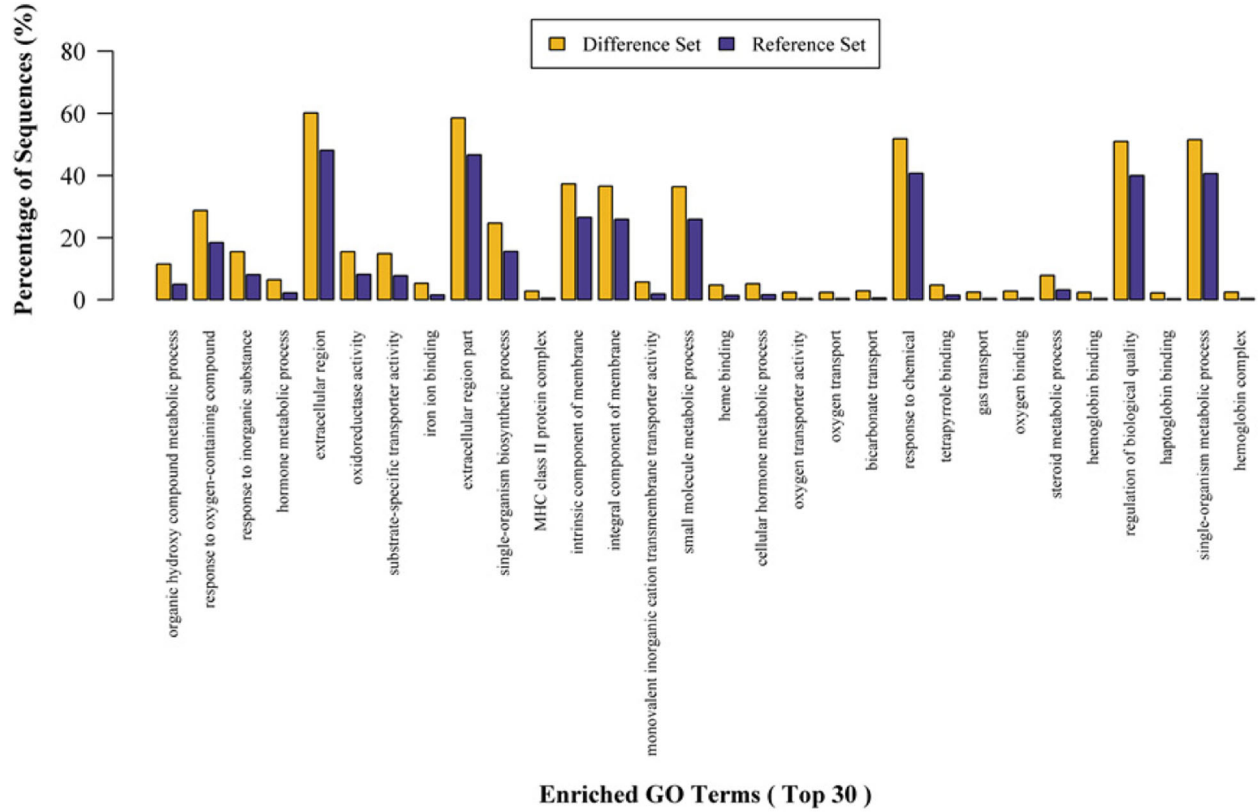

Fig. 2 GO enrichment analysis (Difference set: target protein set; Reference set: background protein set)

Among the 753 DEPs, 347 and 406 proteins were significantly upregulated and downregulated in ACA samples, respectively. The top 16 upregulated proteins included E2F3 protein (Table 1). Of the 16 proteins, keratin was the most upregulated protein, and its level was increased by 3.39-fold in ACA samples. Conversely, 406 proteins were significantly downregulated in ACA samples, and the top 16 downregulated proteins are listed in Table 2.

KEGG pathway analysis

To obtain functional pathway information, we further analyzed the DEPs using the KEGG database. KEGG pathway analysis identified the signaling pathways of DEPs (Figs. 3 and 4).

PPI network of three DEPs

The interaction network of three DEPs between ACA samples and adjacent normal adrenal gland tissue was predicted using the String database (Fig. 5).

Verification of three DEPs by Western blot

We then validated the expression of E2F3, KRT6A, and ALDH1A2 in the abovementioned 24 ACA samples. Western blot analysis revealed that E2F3 and KRT6A expression increased in ACA samples compared with that in adjacent normal adrenal gland tissue (Fig. 6). By contrast, ALDH1A2 expression significantly decreased in ACA samples.

Discussion

iTRAQ is one of the most advanced technology in modern quantitative proteomics [21, 22]; it combines stable isotope labeling with tandem mass spectrometry [23–25] to compare the relative amount of proteins from normal and diseased samples in a single experiment. Wang WS et al. [26] revealed that myoferlin is a novel prognostic predictor in pancreatic adenocarcinoma through iTRAQ-based quantitative proteomics. In the present study, we used this method to detect protein expression changes in ACAs to identify DEPs that are critical for the molecular mechanism. In particular, we conducted GO and pathway analyses to explore the role of upregulated proteins in ACA progression. Selected DEPs (E2F3, KRT6A, and ALDH1A2) were validated by Western blot. This work will provide a valuable basis for further studies in the field of transformative medicine.

Table 1 Top 16 increased expressed proteins in adrenal adenoma compared with normal tissue

Accession	Gene Name	Description	A/B	*P* value
P04259	KRT6B	Keratin, type II cytoskeletal 6B	3.39341	3.45E-24
P08263	GSTA1	Glutathione S-transferase A1	3.29119	4.50E-23
Q499G5	E2F3	E2F3 protein	2.93248	4.08E-19
Q05315	CLC	Galectin-10	2.85897	2.68E-18
P61927	RPL37	60S ribosomal protein L37	2.85584	2.90E-18
P08779	KRT16	Keratin, type I cytoskeletal 16	2.81279	8.77E-18
P04196	HRG	Histidine-rich glycoprotein	2.74085	5.56E-17
A0A0E3DDZ3	HLA-DPB1	MHC class II antigen	2.6654	3.87E-16
Q8NFP4	MDGA1	MAM domain-containing glycosylphosphatidylinositol anchor protein 1	2.34899	1.30E-12
P02741	CRP	C-reactive protein	2.25659	1.37E-11
Q16772	GSTA3	Glutathione S-transferase A3	2.20795	4.70E-11
B2R920		cDNA, FLJ94170	2.11487	4.88E-10
F8TVR8	HLA-DRB1	MHC class II antigen	2.11385	5.01E-10
A7DWG6	HLA-DRB1	MHC class II antigen	2.05556	2.14E-09
Q3T906	GNPTAB	N-acetylglucosamine-1-phosphotransferase subunits alpha/beta	2.03206	3.83E-09
A0A024RB62	METTL1	tRNA (guanine-N(7)-)-methyltransferase	2.02347	4.73E-09

Transcription factor E2F3 is mainly involved in cell proliferation. It participates in transcription repression in quiescent cells by interacting with histone deacetylase and primarily controls genes regulating S phase entry and DNA synthesis. Some studies predicted that E2F3 transcription factor might be a promising biomarker in various cancer and metabolism diseases [27–29]. For instance, to predict overall survival and cause-specific survival in prostate cancer, E2F3 is considered a relatively independent factor [30]. Furthermore, E2F3a stimulates

Table 2 Top 16 decreased expressed proteins in adrenal adenoma compared with normal tissue

Accession	Gene Name	Description	A/B	*P* value
Q9Y639	NPTN	Neuroplastin	0.789565	0.0499304
I7GW38	ND3	NADH-ubiquinone oxidoreductase chain 3	0.789522	0.0498772
Q9H993	ARMT1	Protein-glutamate O-methyltransferase	0.789151	0.0494224
Q8TDY4	ASAP3	Arf-GAP with SH3 domain, ANK repeat and PH domain-containing protein 3	0.788918	0.049138
Q9NRG7	SDR39U1	Epimerase family protein SDR39U1	0.788899	0.0491147
Q16851	UGP2	UTP--glucose-1-phosphate uridylyltransferase	0.78888	0.0490915
Q6UX07	DHRS13	Dehydrogenase/reductase SDR family member 13	0.788815	0.0490121
Q02978	SLC25A11	Mitochondrial 2-oxoglutarate/ malate carrier protein	0.788382	0.0484886
A0A024QZ64	ALDOC	Fructose-bisphosphate aldolase	0.788057	0.048099
H3BQQ1	CMC2	COX assembly mitochondrial protein 2 homolog	0.787879	0.0478859
P34949	MPI	Mannose-6-phosphate isomerase	0.787826	0.047823
P22748	CA4	Carbonic anhydrase 4	0.787682	0.0476521
Q9BTX3	TMEM208	Transmembrane protein 208	0.787579	0.0475292
A0A0S2Z5N0	BEND5	BEN domain containing 5 isoform 1	0.787255	0.0471465
F2YHL7	APOBEC3F	Apolipoprotein B mRNA editing enzyme cytidine deaminase	0.787215	0.0471
Q49B96	COX19	Cytochrome c oxidase assembly protein COX19	0.786704	0.0465007

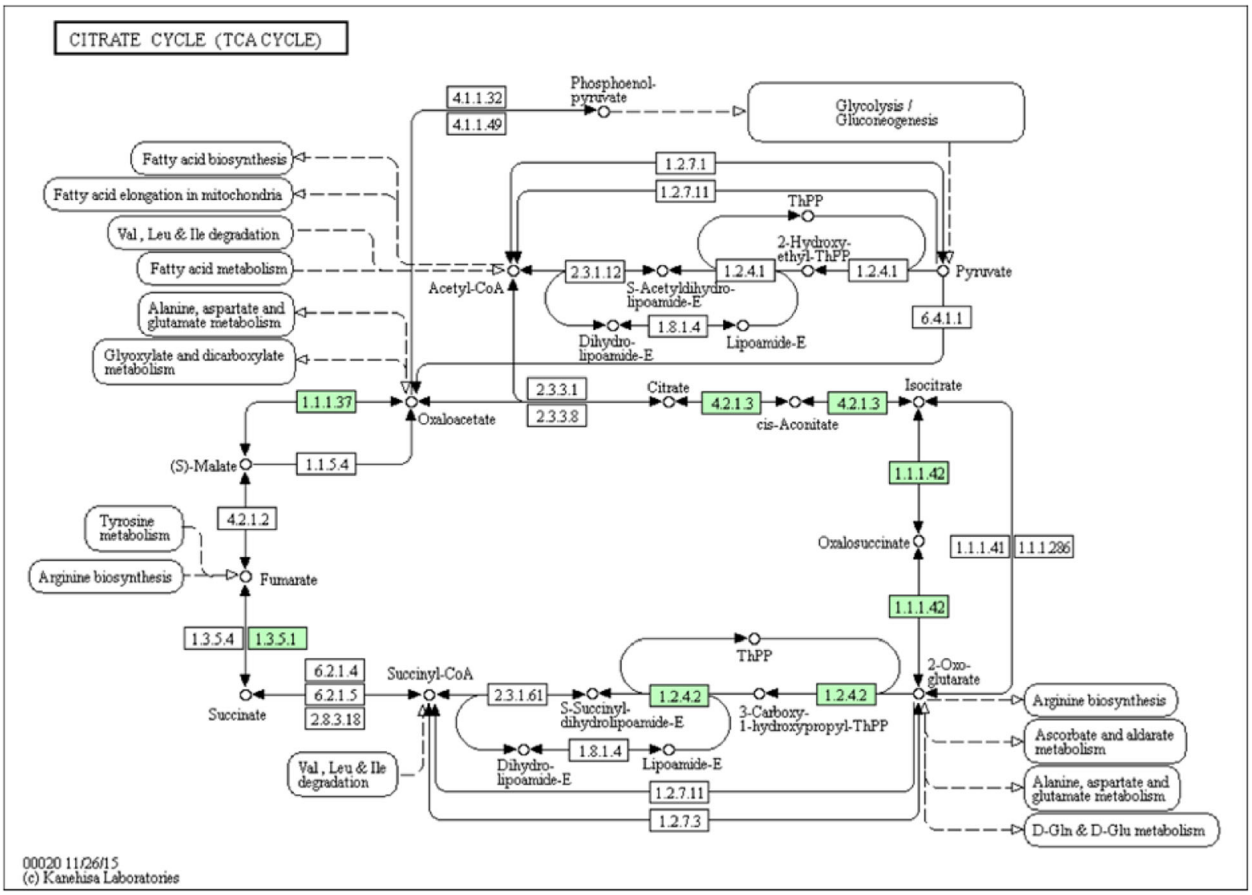

Fig. 3 KEGG pathway functional analysis (The numbers represent the ID of proteins in the KEGG pathway, and the green numbers indicate the ID of differentially expressed proteins)

the proliferation of ovarian cancer cells through EGFR-driven mitogenic cell signals [31]. In lung cancer cells, miR-200b can target E2F3 to lessen cell sensitivity to docetaxel [32]. Martinez et al. [33] revealed that E2F3 is involved in DNA damage-induced apoptosis and can regulate the DNA damage response. Thus, E2F3 is a multifunctional factor that is worth further investigations.

Epidermis-specific type I keratin is generally involved in the activation of follicular keratinocytes after wounding, but it does not play a major role in keratinocyte proliferation or migration. Keratin 6A also participates in the regulation of epithelial migration by inhibiting the activity of SRC during wound repair [34]. Chan JKL et al. [35] verified that manipulating K6a phosphorylation or UPS activity may provide opportunities to harness the innate immunity of epithelia against infection. ALDH1A2 as substrates can recognize free retinal and cellular retinol-binding protein-bound retinal. It mainly metabolizes octanal and decanal but does not metabolize citral, benzaldehyde, acetaldehyde, and propanal efficiently [36, 37]. Shou S et al. [38] revealed that defects in IPCD and digit separation in Hoxa13 mutant mice may be partly caused by reduced levels of RA signaling stemming from a loss in the direct regulation of Aldh1a2.

Besides the proteins we mentioned above, some other studies [39, 40] have revealed that immunohistochemistry detecting CYP11B1 and B2 expression was very promising for patients with primary aldosteronism in establishing a final histopathological diagnosis. We also found CYP11B1 in our differentially expressed protein list, but not in the top 16. This might be due to the individual differences. But we can still pay more attention to this procedure, which could be part of the histopathological routine in all operated primary aldosteronism.

In addition, the discrimination of distinct prognosis between ACA and adrenocortical carcinoma (ACC) deserves our close attention. ACA is a curable neuroendocrine tumor that is usually treated via surgery, whereas ACC is a malignant tumor with a low five-year mortality rate and very poor prognosis [41, 42]. Therefore, future proteomic studies may focus on meaningful markers that allow the differentiation between ACA and

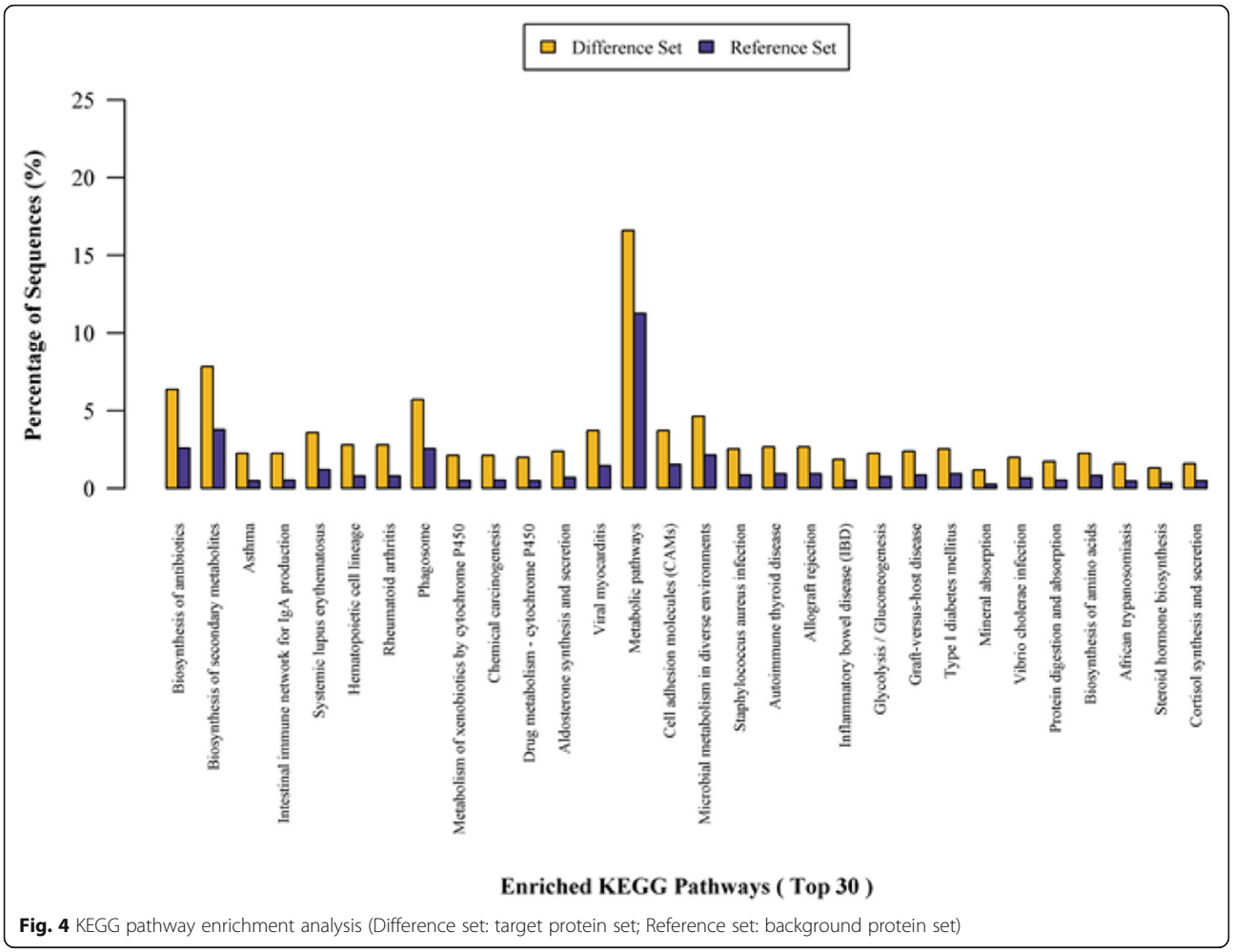

Fig. 4 KEGG pathway enrichment analysis (Difference set: target protein set; Reference set: background protein set)

ACC [6]. An improved understanding of the pathophysiology in these tumors may be obtained by reading lists of hundreds of differentially expressed genes and cellular pathways. There are already some relevant proteomic studies about adrenal cortical tumors [43, 44]. But we still need to go further.

Thus, the PPI network predicted by bioinformatic analysis can provide some useful indications for follow-up scientific research and meaningful clues to explore and detect the binding residues under specific chemical and physical statuses [45–48]. Further improvement is necessary to achieve substantial interactions [49–51]. Developing powerful methods (such as deep neural networks) and obtaining a systematic understanding of the basic mechanisms of PPI require additional time. We hope that the current work will motivate PPI forecasters to conduct further research.

Conclusions

The iTRAQ technique is a powerful tool for the identification of protein isoforms and comparative proteome studies. In this study, we identified 753 DEPs in ACA tissue compared with the control. Further studies are necessary to understand the functions of the identified proteins (E2F3, KRT6A, and ALDH1A2) in ACAs. A better understanding of the mechanisms underlying the upregulation of these proteins may be important for therapeutic purposes in PA due to ACAs.

Methods

Clinical specimens of adrenal adenoma tissue collection

The experimental group randomly collected four clinical specimens of human ACAs from June 2015 to December 2018 in the Second Hospital of Jilin University. The age and gender of all included patients were randomly selected. No adjuvant therapy, such as radiotherapy or chemotherapy, was performed before surgery. ACA tissue was confirmed by pathology after operation. Each patient's tissue was obtained within 30 min after surgical resection and divided into two parts. One tissue was immersed in 4% formalin solution, and the other tissue was stored in sterile nitrogen tubes in liquid nitrogen. The control group was selected from normal adrenal cortex tissues adjacent to the tumorwhich appears

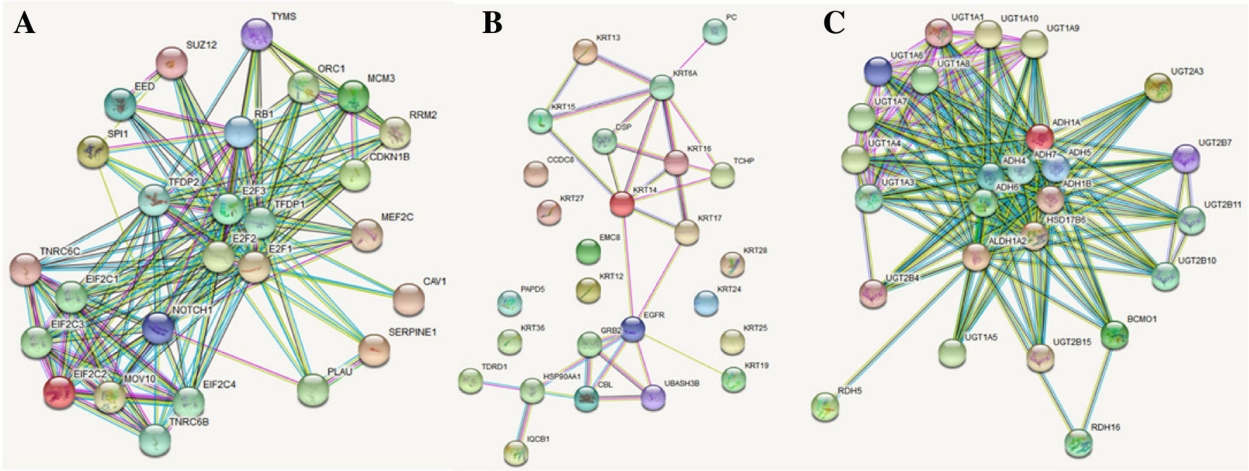

Fig. 5 Protein-protein interaction (PPI) network based on the DEPs-. The round nodes indicate individual proteins. Regulations of protein abundance are shown as red (up-regulation) or green (down-regulation) circles. **a** PPI network based on the up-regulated DEP- E2F3. **b** PPI network based on the down-regulated DEP- KRT6A. **c** PPI network based on the up-regulated DEP- ALDH1A2

normal under the microscope and was confirmed by pathologists in our hospital (Additional file 1: Figure S1). This experimental study was approved by the Ethics Committee of the Second Hospital of Jilin University.

iTRAQ

The detailed procedure has been described previously [52]. In brief, the protein samples were precipitated with acetone–TCA and digested by trypsin to generate proteolytic peptides, which were labeled with iTRAQ reagents. The combined peptide mixtures were analyzed by LC-MS/MS for both identification and quantification. Functional enrichment analysis was performed using GO (http://www.geneontology.org/) for biological process, cellular component, and molecular function. Pathway enrichment analysis of protein clusters was performed by KEGG mapping (http://www.genome.jp/kegg/).

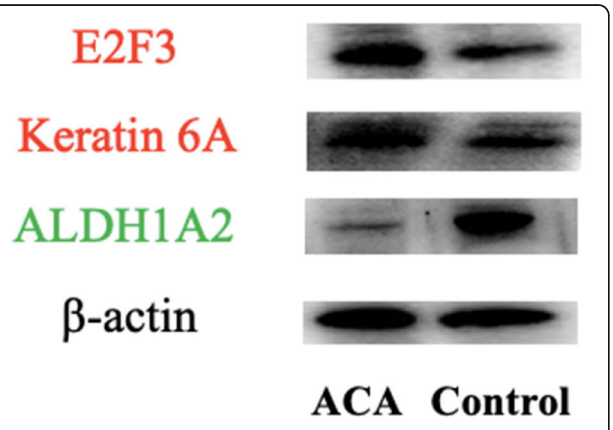

Fig. 6 Representative characteristics of adrenocortical adenomas patients for Western blot validation. E2F3 and KRT6A expression increased in ACA samples compared with that in adjacent normal adrenal gland tissue. By contrast, ALDH1A2 expression significantly decreased in ACA samples

PPI network construction

STRING v10.1 (http://string-db.org/) was applied to analyze the PPI of DEPs identified in the current study and to construct PPI networks. The protein interaction information was extracted from the orthologous proteins of clinical human ACA tissues. The active prediction methods, such as database, experiment, and text mining, were enabled [53].

Western blot

Proteins extracted from patient samples were separated by 10% SDS–PAGE and then transferred to PVDF membranes (Millipore, Bedford, MA, USA). Membranes were blocked for 1 h in Tris-buffered saline containing Tween (TBST; 20 mM Tris–HCl [pH 7.6], 137 mM NaCl, 0.1% Tween-20) and 5% BSA. After incubation with primary antibodies at 4 °C overnight, the membranes were then washed three times with TBST and incubated with horseradish peroxidase (HRP)-conjugated secondary antibodies (anti-rabbit or anti-mouse IgG: 1:4000, Sigma, USA) for 2 h at room temperature. Bound antibodies were detected by HRP-conjugated rabbit anti-mouse antibody. Band density was quantified by ImageJ and normalized to GAPDH.

Statistical analysis

Data are given as the mean ± SEM. GraphPad Prism Software (San Diego, CA, USA) was used for statistical analysis. The significance of differences between groups was determined by a non-paired Student's t-test.

Additional file

Additional file 1: Figure S1. The representative image of medullar-free normal cortex. (DOC 7087 kb)

Abbreviations

ACA: Adrenocortical adenoma; DEPs: Differentially expressed proteins; iTRAQ: Isobaric tags for relative and absolute quantitation; PA: Primary aldosteronism; PPI: Protein–protein interaction

Acknowledgements

Not Applicable.

Authors' contributions

HM, RWL, and KW conducted the literature search and wrote the paper. RWL and KW designed the study, obtained funding, and provided technical support. HM, XD, XJ, YW, BJL, CLS, MSJ, and XRZ participated in the main experiments and collected the data. All authors read and approved the final manuscript.

Funding

This study was supported by the Medical And Health Industry Development Guide Funds of Jilin Province (No. 201603034YY) to **Ke Wang**, the Special funds for Industrial Innovation in Jilin Province (#2016C043–3) to **Ke Wang**, and the Natural Science Foundation of Jilin Province (No. 20180101103JC) to **Ranwei Li**. Ke Wang and Ranwei Li designed the study, obtained funding, provided technical and data support.

Availability of data and materials

All the supporting data are included as additional files.

Ethics approval and consent to participate

This experimental study was approved by the Ethics Committee of the Second Hospital of Jilin University. These patients signed an informed consent form for the experimental study.

Consent for publication

Not applicable.

Competing interests

The authors declare that they have no competing interests.

Author details

[1]Department of Respiratory Medicine, the Second Hospital of Jilin University, Changchun, China. [2]Department of Urinary Surgery, the Second Hospital of Jilin University, Changchun, China. [3]Department of Hematology, the Second Hospital of Jilin University, Changchun, China. [4]Department of Intensive Care Unit, the Second Hospital of Jilin University, Changchun, China. [5]Department of Anesthesiology, the Second Hospital of Jilin University, Changchun, China.

Received: 13 December 2018 Accepted: 12 August 2019
Published online: 16 August 2019

References

1. Galati SJ. Primary aldosteronism: challenges in diagnosis and management. Endocrinol Metab Clin N Am. 2015;44(2):355–69.
2. Weiner ID. Endocrine and hypertensive disorders of potassium regulation: primary aldosteronism. Semin Nephrol. 2013;33(3):265–76.
3. James BB, Adina TF, Richard AJ. Primary Aldosteronism: practical approach to diagnosis and management. Circulation. 2018;138(8):823–35.
4. Zennaro MC, Boulkroun S, Fernandes-Rosa F. Genetic Causes of Functional Adrenocortical Adenomas. Endocr Rev. 2017 Dec 1;38(6):516–37.
5. Calebiro D, Di Dalmazi G, Bathon K, Ronchi CL, Beuschlein F. cAMP signaling in cortisol-producing adrenal adenoma. Eur J Endocrinol. 2015; 173(4):M99–106.
6. Jouinot A, Armignacco R, Assié G. Genomics of benign adrenocortical tumors. J Steroid Biochem Mol Biol. 2019;193:105414.
7. Faillot S, Assie G. ENDOCRINE TUMOURS: The genomics of adrenocortical tumors. Eur J Endocrinol. 2016;174(6):R249–65.
8. Nakamura Y, Yamazaki Y, Felizola SJ, Ise K, Morimoto R, Satoh F, Arai Y, Sasano H. Adrenocortical carcinoma: review of the pathologic features, production of adrenal steroids, and molecular pathogenesis. Endocrinol Metab Clin N Am. 2015;44(2):399–410.
9. Anderson NL, Anderson NG, Pearson TW, Borchers CH, Paulovich AG, Patterson SD, Gillette M, Aebersold R, Carr SA. A human proteome detection and quantitation project. Mol Cell Proteomics. 2009;8(5):883–6.
10. Eckhard U, Marino G, Butler GS, Overall CM. Positional proteomics in the era of the human proteome project on the doorstep of precision medicine. Biochimie. 2016;122:110–8.
11. Sabino F, Hermes O, Egli FE, Kockmann T, Schlage P, Croizat P, Kizhakkedathu JN, Smola H, auf dem Keller U. In vivo assessment of protease dynamics in cutaneous wound healing by degradomics analysis of porcine wound exudates. Mol Cell Proteomics. 2015 Feb;14(2):354–70.
12. Vizovišek M, Vidmar R, Fonović M, Turk B. Current trends and challenges in proteomic identification of protease substrates. Biochimie. 2016;122:77–87.
13. Trinh HV, Grossmann J, Gehrig P, Roschitzki B, Schlapbach R, Greber UF, Hemmi S. iTRAQ-based and label-free proteomics approaches for studies of human adenovirus infections. Int J Proteomics. 2013;2013:581862.
14. Latosinska A, Vougas K, Makridakis M, Klein J, Mullen W, Abbas M, Stravodimos K, Katafigiotis I, Merseburger AS, Zoidakis J, Mischak H, Vlahou A, Jankowski V. Comparative Analysis of Label-Free and 8-Plex iTRAQ Approach for Quantitative Tissue Proteomic Analysis. PLoS One. 2015;10(9):e0137048.
15. Wang H, Alvarez S, Hicks LM. Comprehensive comparison of iTRAQ and label-free LC-based quantitative proteomics approaches using two Chlamydomonas reinhardtii strains of interest for biofuels engineering. J Proteome Res. 2012;11(1):487–501.
16. Sandberg A, Branca RM, Lehtiö J, Forshed J. Quantitative accuracy in mass spectrometry based proteomics of complex samples: the impact of labeling and precursor interference. J Proteome. 2014;96:133–44.
17. Wang H, Li Y, Yang L, Yu B, Yan P, Pang M, Li X, Yang H, Zheng G, Xie J, Guo R. Mass spectrometry-based, label-free quantitative proteomics of round spermatids in mice. Mol Med Rep. 2014;10(4):2009–24.
18. Heroux MS, Chesnik MA, Halligan BD, Al-Gizawiy M, Connelly JM, Mueller WM, Rand SD, Cochran EJ, LaViolette PS, Malkin MG, Schmainda KM, Mirza SP. Comprehensive characterization of glioblastoma tumor tissues for biomarker identification using massspectrometry-based label-free quantitative proteomics. Physiol Genomics. 2014;46(13):467–81.
19. Smits AH, Jansen PW, Poser I, Hyman AA, Vermeulen M. Stoichiometry of chromatin-associated protein complexes revealed by label-free quantitative massspectrometry-based proteomics. Nucleic Acids Res. 2013;41(1):e28.
20. Ashburner M, Ball CA, et al. Gene ontology: tool for the unification of biology. The Gene Ontology Consortium. Nat Genet. 2000;25(1):25–9.
21. Luan X, Cao Z, Xing Z, Liu M, Gao M, Meng B, Fan R. Comparative proteomic analysis of pituitary glands from Huoyan geese between pre-laying and laying periods using an iTRAQ-based approach. PLoS One. 2017; 12(9):e0185253.
22. Unwin RD, Griffiths JR, Whetton AD. Simultaneous analysis of relative protein expression levels across multiple samples using iTRAQ isobaric tags with 2D nano LC-MS/MS. Nat Protoc. 2010;5(9):1574–82.
23. Shum AMY, Poljak A, Bentley NL, Turner N, Tan TC, Polly P. Proteomic profiling of skeletal and cardiac muscle in cancer cachexia: alterations in sarcomeric and mitochondrial protein expression. Oncotarget. 2018; 9(31):22001–22.
24. Jamaluddin MFB, Nagendra PB, Nahar P, Oldmeadow C, Tanwar PS. Proteomic Analysis Identifies Tenascin-C Expression Is Upregulated in Uterine Fibroids. Reprod Sci. 2018;1. https://doi.org/10.1177/1933719118773420.
25. Klimek-Piotrowska W, Krawczyk-Ożóg A, Suski M, Kapusta P, Wołkow PP, Hołda MK. Comparative iTRAQ analysis of protein abundance in the human sinoatrial node and working cardiomyocytes. J Anat. 2018;232(6):956–64.
26. Wang WS, Liu XH, Liu LX, Lou WH, Jin DY, Yang PY, Wang XL. iTRAQ-based quantitative proteomics reveals myoferlin as a novel prognostic predictor in pancreatic adenocarcinoma. J Proteome. 2013;91:453–65.
27. Yang J, Zhang HF, Qin CF. MicroRNA-217 functions as a prognosis predictor and inhibits pancreatic cancer cell proliferation and invasion via targeting E2F3. Eur Rev Med Pharmacol Sci. 2017;21(18):4050–7.
28. Iwahori S, Kalejta RF. Phosphorylation of transcriptional regulators in the retinoblastoma protein pathway by UL97, the viral cyclin-dependent kinase encoded by human cytomegalovirus. Virology. 2017;512:95–103.

29. Trikha P, Sharma N, Pena C, Reyes A, Pécot T, Khurshid S, Rawahneh M, Moffitt J, Stephens JA, Fernandez SA, Ostrowski MC, Leone G. E2f3 in tumor macrophages promotes lung metastasis. Oncogene. 2016;35(28):3636–46.
30. Foster CS, Falconer A, Dodson AR, Norman AR, Dennis N, Fletcher A, Southgate C, Dowe A, Dearnaley D, Jhavar S, Eeles R, Feber A, Cooper CS. Transcription factor E2F3 overexpressed in prostate cancer independently predicts clinical outcome. Oncogene. 2004;23(35):5871–9.
31. Reimer D, Hubalek M, Riedle S, Skvortsov S, Erdel M, Concin N, Fiegl H, Müller-Holzner E, Marth C, Illmensee K, Altevogt P, Zeimet AG. E2F3a is critically involved in epidermal growth factor receptor-directed proliferation in ovariancancer. Cancer Res. 2010;70(11):4613–23.
32. Feng B, Wang R, Song HZ, Chen LB. MicroRNA-200b reverses chemoresistance of docetaxel-resistant human lung adenocarcinoma cells by targeting E2F3. Cancer. 2012;118(13):3365–76.
33. Martinez LA, Goluszko E, Chen HZ, Leone G, Post S, Lozano G, Chen Z, Chauchereau A. E2F3 is a mediator of DNA damage-induced apoptosis. Mol Cell Biol. 2010;30(2):524–36.
34. Lee JT, Wang G, Tam YT, Tam C. Membrane-Active Epithelial Keratin 6A Fragments (KAMPs) Are Unique Human Antimicrobial Peptides with a Non -αβ Structure. Front Microbiol. 2016;7:1799.
35. Chan JKL, Yuen D, Too PH, Sun Y, Willard B, Man D, Tam C. Keratin 6a reorganization for ubiquitin-proteasomal processing is a direct antimicrobial response. J Cell Biol. 2018;217(2):731–44.
36. Zaman TS, Arimochi H, Maruyama S, Ishifune C, Tsukumo SI, Kitamura A, Yasutomo K. Notch Balances Th17 and Induced Regulatory T Cell Functions in Dendritic Cells by Regulating Aldh1a2 Expression. J Immunol. 2017 Sep 15;199(6):1989–97.
37. Kasimanickam VR. Expression of retinoic acid-metabolizing enzymes, ALDH1A1, ALDH1A2, ALDH1A3, CYP26A1, CYP26B1 and CYP26C1 in canine testis during post-natal development. Reprod Domest Anim. 2016;51(6):901–9.
38. Shou S, Carlson HL, Perez WD, Stadler HS. HOXA13 regulates Aldh1a2 expression in the autopod to facilitate interdigital programmed cell death. Dev Dyn. 2013;242(6):687–98.
39. Volpe C, Hamberger B, Zedenius J, Juhlin CC. Impact of immunohistochemistry on the diagnosis and management of primary aldosteronism: an important tool for improved patient follow-up. Scand J Surg. 2019 Jan;17:1457496918822622.
40. Swierczynska MM, Betz MJ, Colombi M, Dazert E, Jenö P, Moes S, Pfaff C, Glatz K, Reincke M, Beuschlein F, Donath MY, Hall MN. Proteomic landscape of aldosterone-producing adenoma. Hypertension. 2019;73(2):469–80.
41. Lerario AM, Moraitis A, Hammer GD. Genetics and epigenetics of adrenocortical tumors. Mol Cell Endocrinol. 2014;386(1–2):67–84.
42. Kirschner LS, Stratakis CA. 5th International ACC Symposium: The New Genetics of Benign Adrenocortical Neoplasia: Hyperplasias, Adenomas, and Their Implications for Progression into Cancer. Horm Cancer. 2016;7(1):9–16.
43. Kim HM, Lee YK, Koo JS. Proteome analysis of adrenal cortical tumors. Expert Rev Proteomics. 2016;13(8):747–55.
44. Yang MS, Wang HS, Wang BS, Li WH, Pang ZF, Zou BK, Zhang X, Shi XT, Mu DB, Zhang DX, Gao YS, Sun XW, Xia SJ. A comparative proteomic study identified calreticulin and prohibitin up-regulated in adrenocorticalcarcinomas. Diagn Pathol. 2013;8:58.
45. Stevers LM, de Vink PJ, Ottmann C, Huskens J, Brunsveld L. A Thermodynamic Model for Multivalency in 14-3-3 Protein-Protein Interactions. J Am Chem Soc. 2018;140(43):14498-510.
46. Taylor IR, Dunyak BM, Komiyama T, Shao H, Ran X, Assimon VA, Kalyanaraman C, Rauch JN, Jacobson MP, Zuiderweg ERP, Gestwicki JE. High-throughput screen for inhibitors of protein-protein interactions in a reconstituted heat shock protein 70 (Hsp70) complex. J Biol Chem. 2018;293(11):4014–25.
47. Jelínek J, Škoda P, Hoksza D. Utilizing knowledge base of amino acids structural neighborhoods to predict protein-proteininteraction sites. BMC Bioinformatics. 2017;18(Suppl 15):492.
48. Wong JH, Alfatah M, Sin MF, Sim HM, Verma CS, Lane DP, Arumugam P. A yeast two-hybrid system for the screening and characterization of small -molecule inhibitors of protein-protein interactions identifies a novel putative Mdm2-binding site in p53. BMC Biol. 2017;15(1):108.
49. Chang JW, Zhou YQ, Ul Qamar MT, Chen LL, Ding YD. Prediction of protein-protein interactions by evidence combining methods. Int J Mol Sci. 2016; 17(11):1946.
50. Keskin O, Tuncbag N, Gursoy A. Predicting Protein-Protein Interactions from the Molecular to the Proteome Level. Chem Rev. 2016;116(8):4884–909.
51. Murakami Y, Tripathi LP, Prathipati P, Mizuguchi K. Network analysis and in silico prediction of protein-protein interactions with applications in drug discovery. Curr Opin Struct Biol. 2017;44:134–42.
52. Wang X, Li Y, Xu G, Liu M, Xue L, Liu L, Hu S, Zhang Y, Nie Y, Liang S, Wang B, Ding J. Mechanism study of peptide GMBP1 and its receptor GRP78 in modulating gastric cancer MDR by iTRAQ-based proteomic analysis. BMC Cancer. 2015;15:358.
53. Szklarczyk D, Franceschini A, Kuhn M, Simonovic M, Roth A, Minguez P, Doerks T, Stark M, Muller J, Bork P, et al. The STRING database in 2011: functional interaction networks of proteins, globally integrated and scored. Nucleic Acids Res. 2011;39(Database issue):D561–8.

Publisher's Note